IEEE Photonics Journal
An IEEE Photonics Society Publication

Open Access

Integral Floating 3-D Display Using Two Retro-Reflector Arrays

Volume 9, Number 2, April 2017

Zi Wang
Anting Wang
Xiaohui Ma
Boyuan Liu
Fenghua Ma
Hai Ming

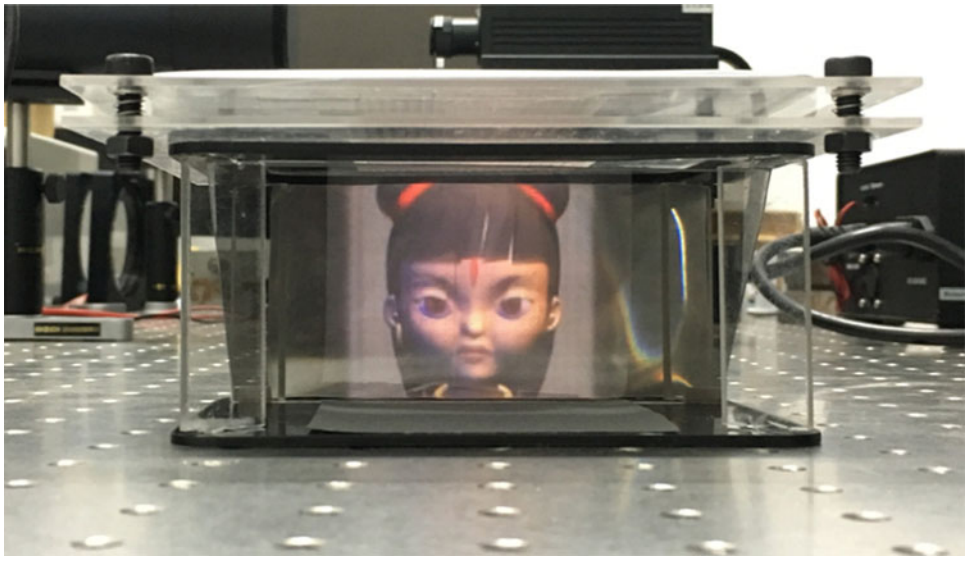

DOI: 10.1109/JPHOT.2017.2683500
1943-0655 © 2017 IEEE

IEEE photonics SOCIETY

IEEE

Integral Floating 3-D Display Using Two Retro-Reflector Arrays

Zi Wang, Anting Wang, Xiaohui Ma, Boyuan Liu, Fenghua Ma, and Hai Ming

Department of Optics and Optical Engineering, Anhui Key Laboratory of Optoelectronic Science and Technology, University of Science and Technology of China, Hefei, Anhui 230026 China

DOI:10.1109/JPHOT.2017.2683500
1943-0655 © 2017 IEEE. Translations and content mining are permitted for academic research only. Personal use is also permitted, but republication/redistribution requires IEEE permission. See http://www.ieee.org/publications_standards/publications/rights/index.html for more information.

Manuscript received February 15, 2017; accepted March 13, 2017. Date of publication March 20, 2017; date of current version April 5, 2017. This work was supported by the Fundamental Research Funds for the Central Universities of China under WK6030000052 and in part by the National Key Basic Research Program of China under 2013CBA01703. Corresponding author: A. Wang (e-mail: atwang@ustc.edu.cn).

Abstract: We propose an integral floating display using two retro-reflector arrays. The proposed method is composed of an integral imaging display, a half mirror, and two retro-reflector arrays. In this paper, the depth-resolution limit and the small complete viewing range for real image in conventional integral imaging are theoretically analyzed, and can be improved much in the proposed method. The floating 3-D image looks of high-quality with smooth surface without the influence of the lens array structure. Experiments are performed to verify the method.

Index Terms: Integral imaging, floating display, retro-reflector array.

1. Introduction

Integral imaging (InIm) is a promising technique for achieving glasses-free 3-D display which has a long history [1]. A pinhole array or a lens array is used to record and reconstruct light rays of different directions in space. It has many advantages such as reconstructing 3-D images with full-parallax and a quasi-continuous viewing points. In addition, it can induce observer accommodation cues and provide smooth motion parallax. Due to the great development of high resolution display and detector, InIm revived in the past decades and the existing problems such as low resolution, narrow viewing angle and limited depth range have been effectively improved in a variety of research [2]–[7].

Integral floating display is a 3-D display system which combines integral imaging and floating display [8]–[10]. The previous integral floating display methods used a large convex lens to produce a 3-D image with great feel of depth by forming a real image of the 3-D image integrated by the InIm technique. However, this kind of integral floating display suffers from problems such as narrow viewing window [8], imaging aberration of large-diameter floating lens, and deformed shape of floating image [10].

Floating image can also be generated by an afocal lens array, a roof mirror grid array or a retro-reflector array (RRA) [11], [12]. The scheme producing floated images based on a RRA is easy to implement. It consists of image sources, a half mirror and a RRA. The corner cube array is an example of RRA. A corner cube consists of three mirror planes orthogonalized mutually and

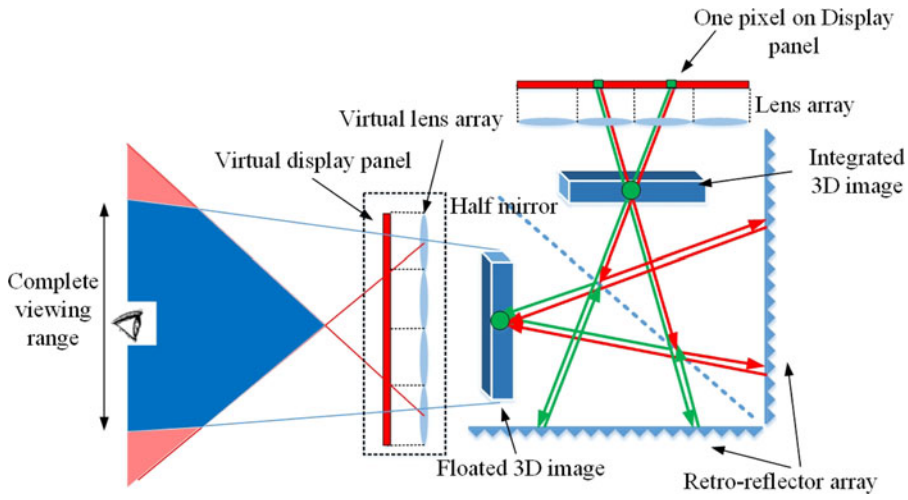

Fig. 1. Proposed scheme producing floated 3-D images.

reverses the direction of incoming light. The RRA consists of a large number of retro-reflectors arranged on a 2-D surface, the size of which is very small. T. Iwane proposed to combine retro-reflection material and light-field display to generate aerial 3-D image [13], [14]. The structure of the light-field display is the reverse of that of a light-field camera [15]. The 3-D scene acquired by a light-field camera will be reconstructed nearby the lens array in light-field display and is not conjugated with display device. Choi proposed to use retro-reflector film to enhance the visibility of pinhole-type integral imaging [16].

We propose an integral floating 3-D display using two RRAs to eliminate the depth-resolution limit and enlarge the complete viewing range for real image in InIm. Compared to integral floating display using a floating lens, the proposed method doesn't have the problems of viewing window, imaging aberration of large-diameter floating lens and deformed shape of floating image.

2. Principle

Schematic diagram of proposed integral floating display is shown in Fig. 1. It is composed of an integral imaging system, a half mirror and 2 RRAs which are corner cube arrays. The integral imaging system consisting of a display panel and a lens array produces the 3-D image. The 3-D image consists of many integrated voxels. Each voxel can be thought as an image source and emits light. Half of the light emitted from the voxel is reflected by the half mirror and the other half transmits through the half mirror. The reflected light is retro-reflected by the RRA and further transmits through the half mirror to form a floated voxel. The transmitted light is retro-reflected by the RRA and further reflected by the half mirror to form the same floated voxel. Two RRAs are used instead of one to improve the optical efficiency. Therefore, a floated 3-D image is reproduced in mid-air. Since many people expects 3-D image reconstructed in space not on screen, this method is more attractive than conventional InIm because viewers dont feel the presence of screen. In addition, the depth-resolution limit and small complete viewing range for real image in conventional InIm can be improved.

2.1 Depth-Resolution Limit

As is well-known, there are two kinds of projection types according to the gap between the display panel and the lens array, called resolution-priority InIm (RPInIm) and depth-priority InIm (DPInIm) [17]. RPInIm has high resolution and low depth range, while DPInIm has low resolution and high

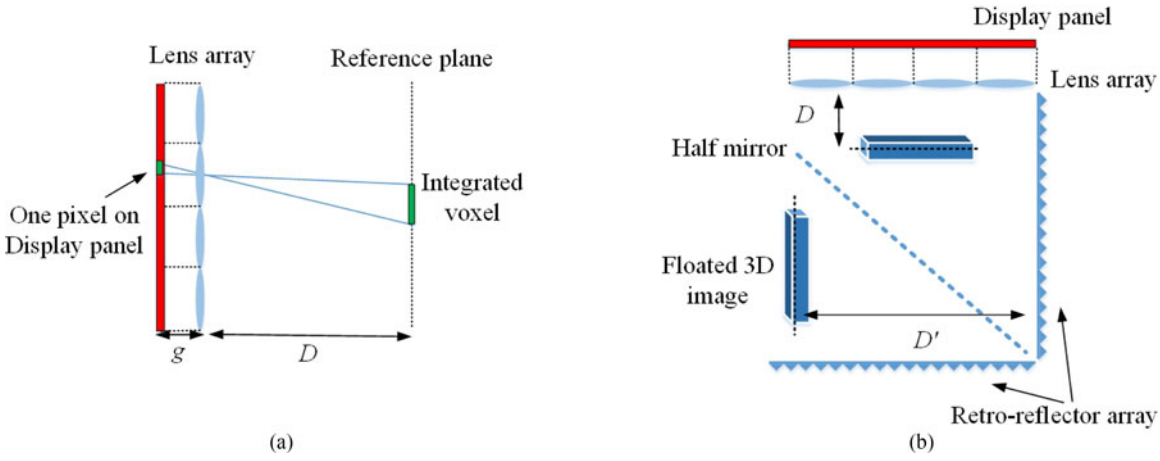

Fig. 2. (a) Depth-resolution limit in conventional InIm. (b) Proposed method eliminates the depth-resolution limit by converting image depth from D to D'.

depth range. Since resolution is the most important factor related to viewers' assessment of a 3-D display technique, RPInIm is more practical and attractive.

In the RPInIm, there exists a privileged plane in the reconstruction space which is focused on by viewer's eyes, the so-called image reference plane (IRP), which is conjugated with the display panel. As shown in Fig. 2(a), the resolution R at IRP in conventional RPInIm is

$$R = g/SD \tag{1}$$

where g denotes distance between display panel and lens array, and S denotes the display pixel size, and D denotes distance between lens array and IRP. The IRP is the plane at which 3-D images locate, and therefore, D is the 3-D image depth. As shown in (1), resolution R is inversely proportional to depth D, that is, resolution decreases as depth increases. To get high viewing resolution, the 3-D image depth should be decreased, which means the integrated 3-D images locate near the screen (lens array), giving the viewer few feeling of depth. But in 3-D display, image depth is also an important factor since a large depth produces impressive feelings, and makes viewers' eyes' focus plane far away from the screen. And the viewers will not feel the presence of screen and will feel that the 3-D image is floating in mid-air.

The depth-resolution limit relation can be removed in Fig. 2(b). In the scheme, the image depth is converted from D to D', which is the distance between floated 3-D image and RRA. The image depth D' can be increased by moving the InIm system far away, without decreasing resolution.

2.2 Complete Viewing Range for Real Image

In RPInIm, there exist two display mode: real mode and virtual mode. In real mode, real images are generated in front of the screen, with g_1 larger than the focal length of lens array. In virtual mode, virtual images are generated behind the screen, with g_2 smaller than the focal length of lens array. The viewing angle without crosstalk is given by

$$\theta = 2tan^{-1}(d/2g) \tag{2}$$

where d is the elemental lens pitch. Since g_1 is larger than g_2, real mode has narrower viewing angle than virtual mode. On the contrary, according to (1), real mode has higher resolution than virtual mode, so there is a trade-off here. Next, we assume g_1 equal to g_2 to discuss the viewing region in real mode and virtual mode.

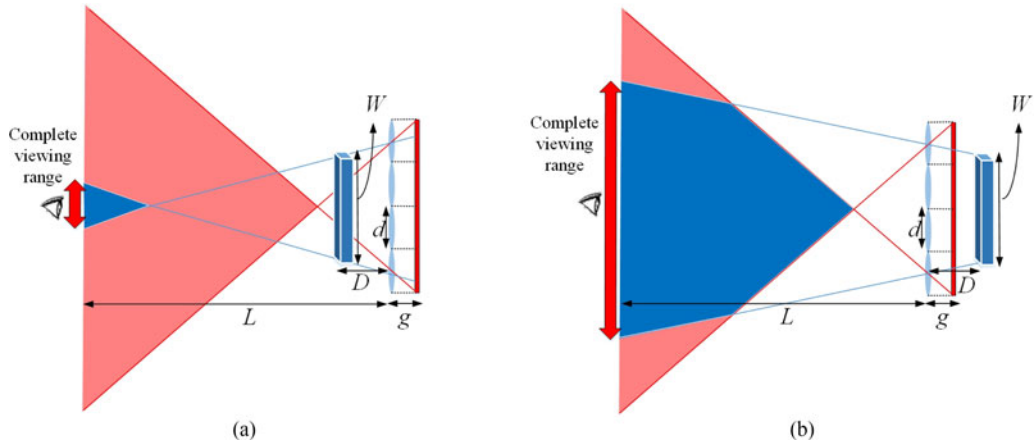

Fig. 3. Complete viewing range only in which the whole 3-D image can be viewed without loss, indicated by red two-way arrow in (a) real mode and (b) virtual mode.

Equation (2) gives the expression of viewing angle without considering the image width and depth. In actual, image width and depth influence the size of viewing range. As shown in Fig. 3, the 3-D image is represented by the blue cuboid for simplicity. Assuming $g_1 = g_2 = g$, the red-colored sections show the viewing region given by (2), and the blue-colored sections show the actual viewing region considering the image width W and depth D. The image width is the lateral size of 3-D images and is represented by the length of the blue cuboid. Viewers inside the red-colored sections don't see crosstalk, but only inside the blue-colored sections can viewers see the whole 3-D image without loss. At a given viewing distance L, the red two-way arrow in Fig. 3 indicates the viewing range in which viewers can see the whole 3-D image without loss. So we refer to it as complete viewing range (CVR).

As shown in Fig. 3, virtual mode has much larger CVR than real mode. The size of CVR A_1 in real mode is given by

$$A_1 = \begin{cases} 0, & L \le \dfrac{(N-1)dD}{(N-1)d - W} \\ \dfrac{L\,[(N-1)d - W]}{D} - (N-1)d, & L > \dfrac{(N-1)dD}{(N-1)d - W} \end{cases} \tag{3}$$

where N is the number of the elemental lenses and L is the viewing distance. The size of CVR A_2 in virtual mode is given by

$$A_2 = \begin{cases} 0, & L \le (N-1)g \\ \dfrac{[L - (N-1)g]d}{g}, & (N-1)g < L \le \frac{2(N-1)d}{\frac{d}{g} - \frac{(N-1)d-W}{D}} \\ \dfrac{L\,[(N-1)d - W]}{D} + (N-1)d, & L > \frac{2(N-1)d}{\frac{d}{g} - \frac{(N-1)d-W}{D}} \end{cases} \tag{4}$$

Fig. 4 shows the size of A_1 and A_2 when D and W change. The value of CVR in the figure is already normalized by the lateral viewing range of the red-colored section in Fig. 3. The other parameters are set as follows: $N = 20$, $d = 2.5$ mm, $g = 7.6$ mm, and $L = 400$ mm. D changes from 40 mm to 139 mm and W changes from 10 mm to 49 mm. It can be seen that A_1 decreases fast to zero as D and W increase. But A_2 only decreases at very large value of D and W. Fig. 4 confirms that virtual mode has much larger CVR than real mode. And it can be seen that the different sizes of CVR in real and

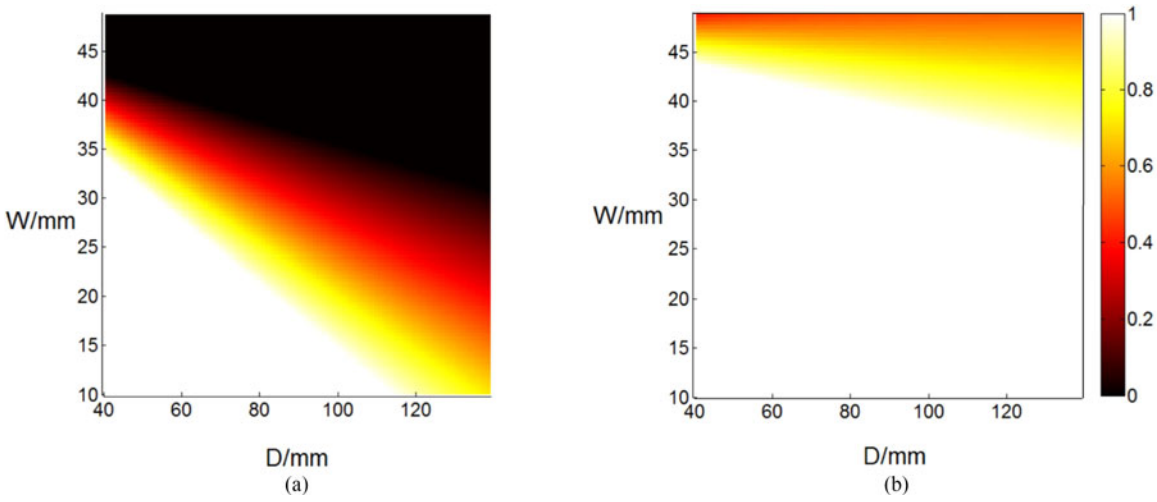

Fig. 4. Normalized size of CVR with image depth D changing from 40 mm to 139 mm and image width W changing from 10 mm to 49 mm in (a) real mode and (b) virtual mode. ($N = 20$, $d = 2.5$ mm, $g = 7.6$ mm, and $L = 400$ mm)

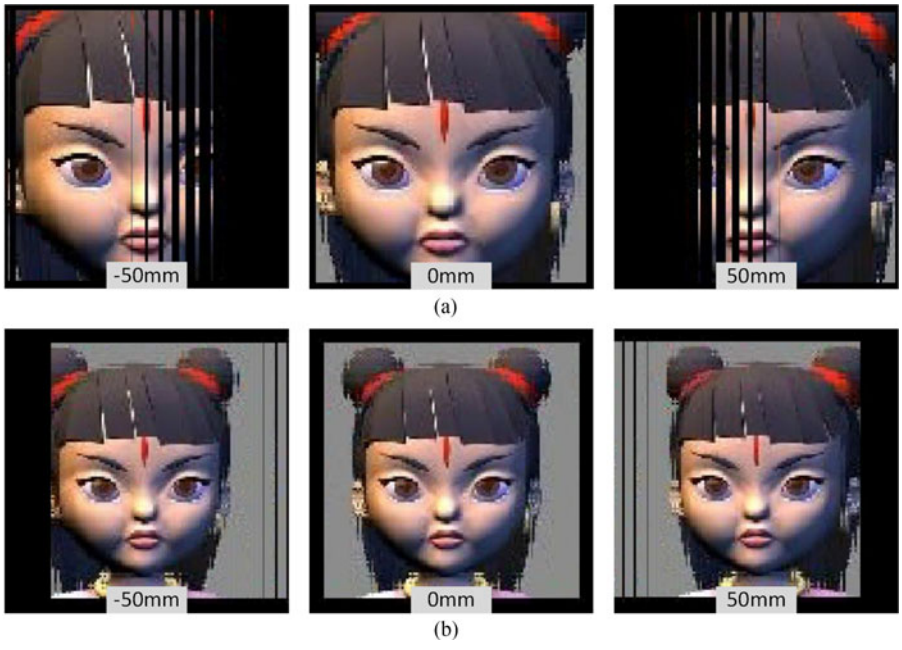

Fig. 5. Visualization simulation results with virtual camera at different lateral positions in (a) real mode and (b) virtual mode.

virtual mode come from the different relative positions between the 3-D image and the lens array. To show the influences of the small CVR in real mode InIm, computational InIm reconstruction using MATLAB has been done. The elemental image array of a cartoon model is generated using the 3-DS MAX modeling software. The smart pseudoscopic-to-orthoscopic conversion algorithm [18] is used to set the image depth to be 60 mm and − 60 mm in real mode and virtual mode respectively. The gaps between elemental image array and lens array in real mode and virtual mode are set equal to be 7 mm. The lens array consists of 20 × 20 elemental lenses with pitch of 2.5 mm. Visualization simulation results are shot by a virtual camera at $L = 400$ mm and are shown in Fig. 5.

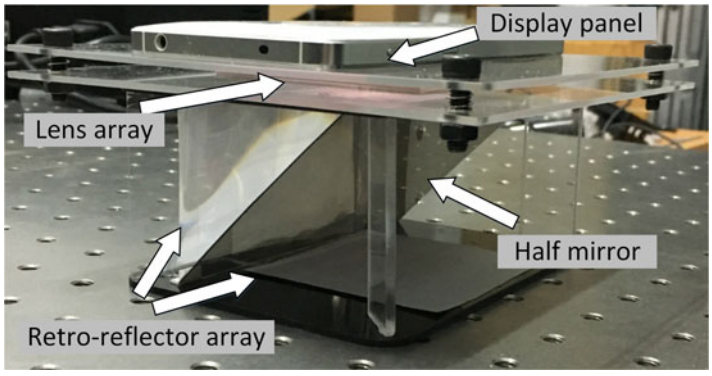

Fig. 6. Experimental setup of proposed method.

The 3-D image in real mode looks larger than that in virtual mode because of smaller distance to the virtual camera. Due to the limit of the small CVR, the 3-D image can't be viewed completely in real mode compared with virtual mode. In addition, as the virtual camera moves laterally, serious information loss appears, which is not apparent in virtual mode. Since the real image is generated in front of the screen, viewers can touch it in the space and vivid interaction can be realized, which makes real mode InIm more preferred than virtual mode InIm. But the CVR for real image is much smaller than that for virtual image, which is a shortcoming need to overcome. The proposed method can increase the CVR for real image to be equal to that for virtual image in conventional InIm by reversing the relative position between 3-D images and lens array.

As shown in Fig. 1, the original 3-D image and the floated 3-D image are image symmetrical to the half mirror. A virtual lens array and a virtual display panel can be thought to exist in front of the floated 3-D image, which is very similar to the case of virtual mode InIm shown in Fig. 3(b). So the small CVR for real image is converted to be equal to that for virtual image in conventional InIm. The conversion of the CVR size comes from the reversal of the relative position between the floated 3-D image and the virtual lens array. Therefore, a real 3-D image with enlarged CVR is generated.

3. Experiment

Optical visualization experiments are performed to verify the feasibility. The experimental setup of the proposed floating InIm is shown in Fig. 6. It consists of a display panel, a lens array, a half mirror and two RRAs. The conventional InIm consisting of a display panel and a lens array generates a real 3-D image in front of the screen with a small CVR. Then a mirror-like floated 3-D image is reproduced in the front of the device through the half mirror and the two RRAs.

Fig. 7(a) and (b) show the observed results in real mode and virtual mode respectively, which are the same as Fig. 5(a) and (b). Fig. 7(c) shows the result of the proposed floating InIm, verifying that the proposed method converts the small CVR for real image to be equal to that for virtual image in conventional InIm. The brightness in the proposed method is low because only half of light is utilized by the half mirror. But the problem can be solved by a reflective polarizer and a quarter wavelength plate [13], [14]. The lens array structure which is very apparent in Fig. 7(a) and (b) is not found in Fig. 7(c), because in conventional InIm, the 3-D images are viewed directly through the lens array in daylight, and the lens array reflects light to viewers eyes, which influence the 3-D images as grid structure, but in the proposed system, the lens array is mounted inside it, reflecting little light. Viewers see the reproduced 3-D images through the half mirror and the retro-reflector arrays, and the lens array can hardly be noticed. Therefore, the 3-D image looks high-quality with smooth surface, and the 3-D image looks like floating in the air but not generated by a screen.

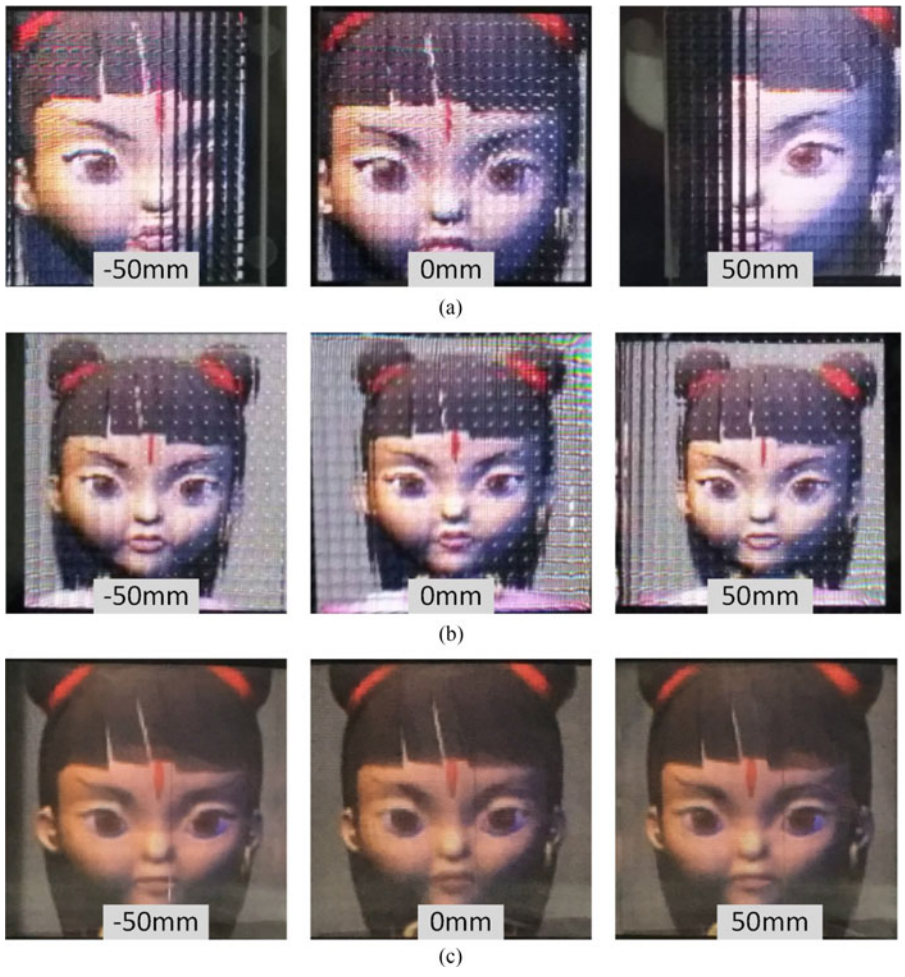

Fig. 7. Optical visualization experiment results with camera at different lateral positions in (a) real mode in conventional InIm, (b) virtual mode in conventional InIm, and (c) proposed method.

4. Conclusion

An integral floating display using two retro-reflector arrays is proposed. The proposed method is composed of an integral imaging display, a half mirror and two retro-reflector arrays. In the proposed method, the depth-resolution limit in conventional InIm is eliminated and the complete viewing range for real image is enlarged much. The floating 3-D image looks high-quality with smooth surface without the influence of the lens array structure. Simulations and experiments are performed to verify the method.

References

[1] G. Lippmann, "Epreuves reversibles. photographies integrals," *Comptes-Rendus Academie des Sci.*, vol. 146, pp. 446–451, 1908.
[2] J.-S. Jang and B. Javidi, "Improved viewing resolution of three-dimensional integral imaging by use of nonstationary micro-optics," *Opt. Lett.*, vol. 27, no. 5, pp. 324–326, 2002.
[3] B. Lee, S. Jung, and J.-H. Park, "Viewing-angle-enhanced integral imaging by lens switching," *Opt. Lett.*, vol. 27, no. 10, pp. 818–820, 2002.
[4] Y. Kim *et al.*, "Depth-enhanced integral imaging display system with electrically variable image planes using polymer-dispersed liquid-crystal layers," *Appl. Opt.*, vol. 46, no. 18, pp. 3766–3773, 2007.

[5] J.-H. Jung, S.-g. Park, Y. Kim, and B. Lee, "Integral imaging using a color filter pinhole array on a display panel," *Opt. Exp.*, vol. 20, no. 17, pp. 18744–18756, 2012.
[6] Y. Oh, D. Shin, B.-G. Lee, S.-I. Jeong, and H.-J. Choi, "Resolution-enhanced integral imaging in focal mode with a time-multiplexed electrical mask array," *Opt. Exp.*, vol. 22, no. 15, pp. 17620–17629, 2014.
[7] Z. Wang, A. Wang, S. Wang, X. Ma, and H. Ming, "Resolution-enhanced integral imaging using two micro-lens arrays with different focal lengths for capturing and display," *Opt. Exp.*, vol. 23, no. 22, pp. 28970–28977, 2015.
[8] J. Kim, S.-W. Min, and B. Lee, "Viewing region maximization of an integral floating display through location adjustment of viewing window," *Opt. Exp.*, vol. 15, no. 20, pp. 13023–13034, 2007.
[9] S.-W. Min, M. Hahn, J. Kim, and B. Lee, "Three-dimensional electro-floating display system using an integral imaging method," *Opt. Exp.*, vol. 13, no. 12, pp. 4358–4369, 2005.
[10] J. Kim, S.-W. Min, and B. Lee, "Floated image mapping for integral floating display," *Opt. Exp.*, vol. 16, no. 12, pp. 8549–8556, 2008.
[11] S. Maekawa, K. Nitta, and O. Matoba, "Advances in passive imaging elements with micromirror array," *Proc SPIE*, vol. 6803, 2008, Art. no. 68030B.
[12] H. Yamamoto, Y. Tomiyama, and S. Suyama, "Floating aerial led signage based on aerial imaging by retro-reflection (AIRR)," *Opt. Exp.*, vol. 22, no. 22, pp. 26919–26924, 2014.
[13] T. Iwane, "Light-field displays and light-field optics," in *Proc. IEEE 15th Workshop Inf. Opt.*, 2016, pp. 1–3.
[14] T. Iwane, M. Nakajima, and H. Yamamoto, "Light-field display combined with an aerial image display device, aerial imaging by retro-reflection (AIRR)," in *Proc. 3-D Image Acquisition Display: Technol., Perception Appl., Opt. Soc. Amer.*, 2016, Paper. TM3A–3.
[15] R. Ng, M. Levoy, M. Brédif, G. Duval, M. Horowitz, and P. Hanrahan, "Light field photography with a hand-held plenoptic camera," *Comput. Sci. Tech. Rep. CSTR*, vol. 2, no. 11, pp. 1–11, 2005.
[16] S. Choi, S.-W. Min, and Y. M. Kim, "Visibility enhancement of pinhole-type integral imaging using retroreflector film," in *Proc. Imag. Syst. Appl., Opt. Soc. Amer.*, 2015, Paper. JTH3A–4.
[17] H. Navarro, R. Martínez-Cuenca, A. Molina-Martian, M. Martínez-Corral, G. Saavedra, and B. Javidi, "Method to remedy image degradations due to facet braiding in 3d integral-imaging monitors," *J. Display Technol.*, vol. 6, no. 10, pp. 404–411, 2010.
[18] H. Navarro, R. Martínez-Cuenca, G. Saavedra, M. Martínez-Corral, and B. Javidi, "3d integral imaging display by smart pseudoscopic-to-orthoscopic conversion (spoc)," *Opt. Exp.*, vol. 18, no. 25, pp. 25573–25583, 2010.